water

Article

Improved Drinking Water Disinfection with UVC-LEDs for *Escherichia Coli* and *Bacillus Subtilis* Utilizing Quartz Tubes as Light Guide

Andrej Gross *, Felix Stangl, Katharina Hoenes, Michael Sift and Martin Hessling *

Institute of Medical Engineering and Mechatronics, Ulm–University of Applied Sciences, Ulm 89081, Germany; E-Mails: stangl@hs-ulm.de (F.S.); hoenes@hs-ulm.de (K.H.); msift@outlook.com (M.S.)

* Authors to whom correspondence should be addressed; E-Mails: angross@mail.hs-ulm.de (A.G.); hessling@hs-ulm.de (M.H.); Tel.: +49-07-3128-568 (A.G. & M.H.).

Abstract: A new approach is investigated utilizing light guidance capabilities of optical pure quartz glass in order to maximize drinking water disinfection efficiency with UVC-light-emitting diodes (LEDs). Two experimental setups consisting of soda-lime AR® glass (VWR, Darmstadt, Germany) or HSQ® 100 quartz glass (Heraeus, Wasserburg, Germany) reactors were designed to compare disinfection rates with and without total reflection of UVC radiation along the reactor walls. Each reactor was filled with 9 mL bacteria samples containing either *E. coli* DSM (Deutsche Sammlung von Mikroorganismen) 498 or *B. subtilis* DSM 402 strains (concentration $1-3 \times 10^6$ colony forming units (CFU)/mL) with and without additional mixing and irradiation periods of 10, 40, and 90 s. Disinfection rates were increased up to 0.95 $\log_{10}$ (*E. coli*) and 0.75 $\log_{10}$ (*B. subtilis*) by the light guide approach in stagnant samples. The same experiments with mixing of the samples resulted in an increased disinfection efficiency of 3.07 $\log_{10}$ (*E. coli*) and 1.59 $\log_{10}$ (*B. subtilis*). Optical calculations determine that total reflection is achieved with the applied UVC-LED's viewing angle of 15°. Furthermore measurements show that HSQ® 100 quartz has a transmittance of 92% at 280 nm UVC irradiation compared to the transmittance of soda-lime glass of 2% (1 mm wall thickness).

Keywords: drinking-water; disinfection; UVC-light guidance; UVC-disinfection reactor

1. Introduction

Contaminated drinking water is an often underestimated problem in First World countries because of the advanced disinfection methods in modern sewage plants and specialized facilities. However, nearly 2.5 billion people worldwide have no access to improved sanitation and 748 million of them still lack sufficient access to improved drinking water sources [1], accounting for over 1.7 million deaths a year, especially in developing countries [2,3]. The upcoming technology of UVC-LEDs promises new inexpensive, environmentally friendly, and long-life disinfection systems for drinking water that can be used decentralized in combination with photovoltaic systems [3]. UVC radiation (200–280 nm) in general is a very efficient way of inactivating pathogen bacteria in drinking water by directly damaging the DNA [4]. Radiation of this wavelength range is able to enter the cell walls of microorganisms and is partly absorbed by the DNA. By this process, thymine dimers are formed, which prevent further replication of the DNA strains [5]. These thymine dimers arise when an UVC photon gets absorbed by adjacent thymine nucleotides, merging them as shown in Figure 1b. A preferable wavelength for disinfection would therefore be expected at about 270 nm, which is the absorption peak of thymine [6,7].
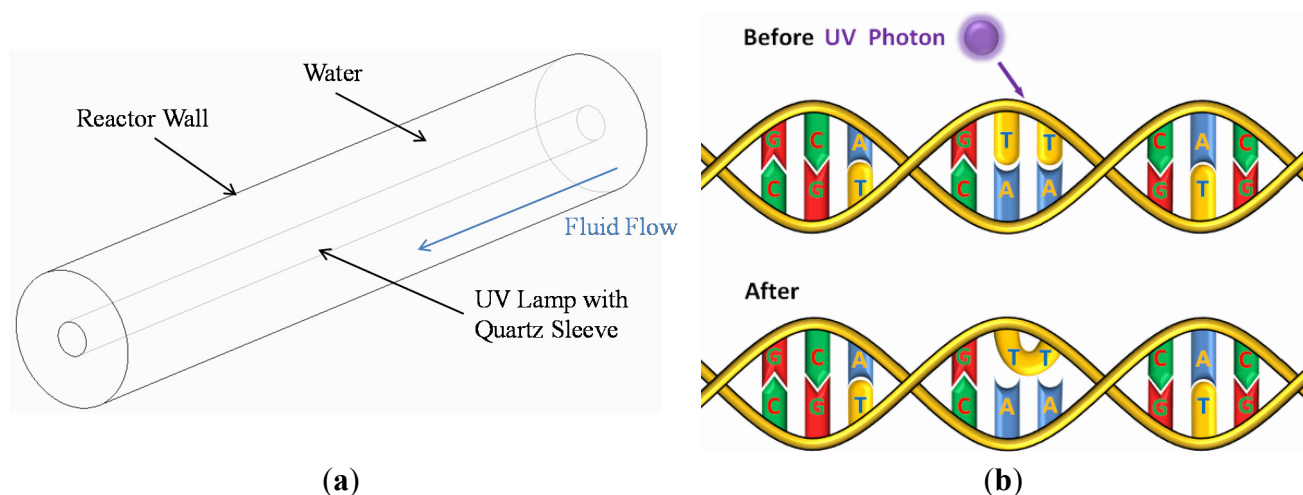

(**a**)   (**b**)

Figure 1. (**a**) Cylindrical UV disinfection closed vessel reactor with mercury vapor lamp; (**b**) formation of thymine dimers by UVC radiation [8].

Today, commercial UV disinfection systems usually apply highly toxic and environmentally harmful low or medium pressure mercury vapor lamps, which have high optical output powers of several watts and a wavelength peak commonly in the UVC range of 254 nm [5,6]. Normally, much UVC power of such a system is wasted due to inadequate optical coupling. Because of the high power output, these systems still guarantee sufficient fluence rates of over 40 mJ/cm^2 [3,5]. Figure 1a shows a buildup concept for a traditional cylindrical UV disinfection reactor [9]. The water flows alongside a mercury vapor lamp and is exposed to UVC-radiation on its way through the reactor. Because of the elongated construction of mercury lamps and the small dimensions of LEDs, this reactor design would be insufficient when applying only a single UVC-LED. However, there are approaches to take over this reactor concept with several UVC-LEDs placed alongside the reactor [10,11]. The questionable environmental and toxic properties of mercury require adequate replacement technologies. In this context, deep UV-LEDs are a promising development and may be able to function as a substitute for

mercury lamps in the near future. However, commercially available UVC-LEDs usually produce severely lower radiant output powers of mostly less than 3 mW [12], thus new and more efficient reactor concepts should be considered.

In order to create sufficient inactivation rates of at least three $\log_{10}$ levels, all of the generated UVC-LED radiation has to be harvested in a novel reactor design. Aiming at very high efficiency, a new concept was created by coupling an UVC-LED in parallel to a quartz tube and keeping UVC radiation inside the tube due to total reflection at the walls. With this approach, most of the optical power is available for disinfection along the whole reactor if certain boundary conditions are met [13]. If normal soda-lime or silicate-based glass types, instead of quartz glass, are used in such a reactor design, the incoming UVC-rays will be absorbed almost completely at the walls. As a result, optical power is wasted and will no longer be available for inactivating microorganisms. A round pipe geometry is analyzed and applied for experimental setup in this work in order to verify the basic capabilities and benefits of this novel reactor design. If this concept proves to be effective, further optimized reactor designs according to this concept, especially for flow reactors, can be considered in future studies.

2. Materials and Methods

2.1. Experimental Setup

An experimental setup allowing precise comparison of the disinfection with and without the concept of total reflection was designed. A schematic view can be seen in Figure 2, with both setups following the same buildup concept. The experiment consists of a glass tube each (either HSQ® 100 quartz from Heraeus (Wasserburg, Germany) or AR® soda-lime glass from VWR (Darmstadt, Germany)), 9 mL distilled water with inserted microorganisms (*E. coli* DSM 498 or *B. subtilis* DSM 402, concentration $1-3 \times 10^6$ colony forming units (CFU)/mL), and an UVC-LED type OPTAN280J from Crystal IS (Green Island, NY, US) delivering a measured radiant output of 0.97 mW (forward voltage: *ca.* 9 V; driving current: 100 mA; power dissipation: 0.9–1 watt) at a measured emission wavelength peak of 281.8 nm. The power supply TOE 8733 from Toellner (Herdecke, Germany) ensured correct voltage and current ratings during all experiments. Both glass tubes were identical except for their material with the dimensions of 12 mm (inner diameter), 14 mm (outer diameter), and a length of 100 mm.

For disinfection, the bacteria solution was exposed to UVC radiation in defined time intervals of 10, 40 and 90 s or doses of 8.64 mJ/cm², 34.59 mJ/cm², and 77.82 mJ/cm², respectively. The bacteria solution inside the tube was mixed continuously with a MR 1000 magnetic stirrer from Heidolph (Schwabach, Germany). Additionally, stagnant experiments without mixing were performed. Because of the attenuation of UVC radiation along the glass tube, the bacteria solution close to the LED was exposed to much higher UVC doses than at the bottom.
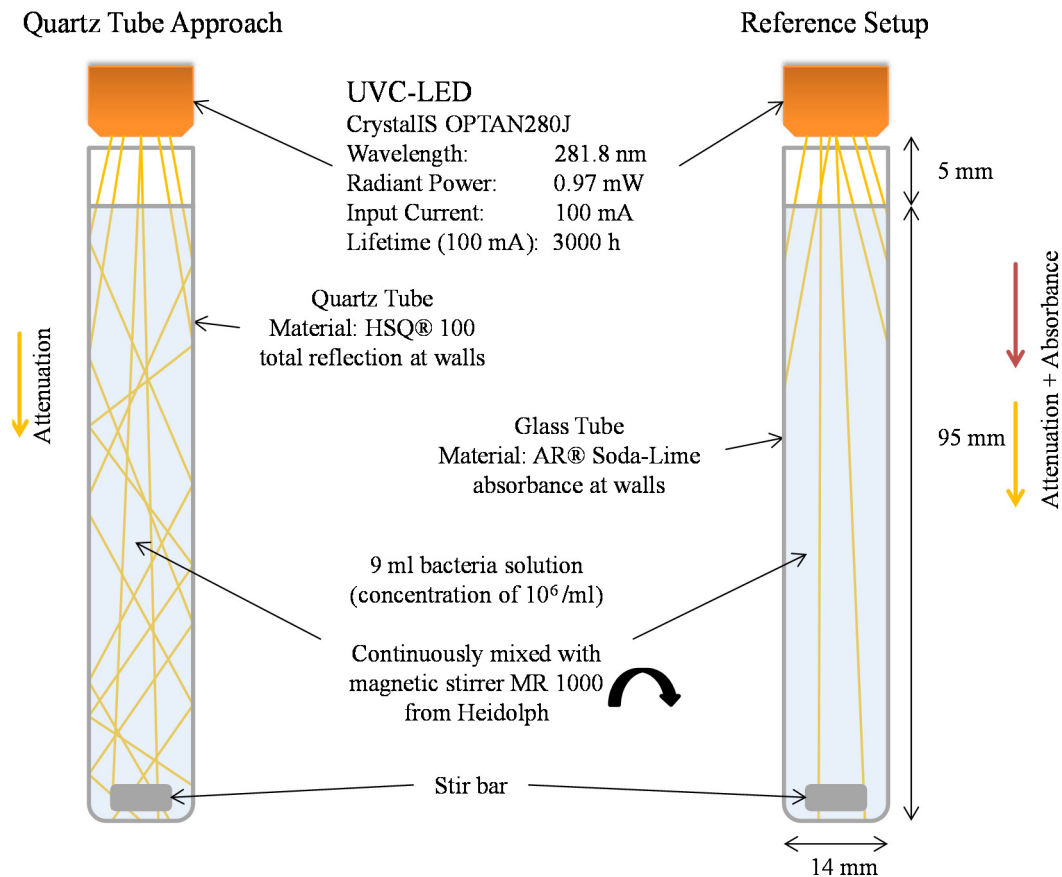
Figure 2. Schematic illustration of the designed experimental setup: (**left**) novel approach utilizing HSQ® 100 quartz glass for total reflection and (**right**) reference setup with AR® glass for quantification of the disinfection enhancements of this concept.

2.2. Bacterial Strains and Growth Conditions

Two different non-pathogenic bacterial strains were applied for the experimental setup, *Escherichia coli* DSM 498 and *Bacillus subtilis* DSM 402. All bacterial strains were from DSMZ (Deutsche Sammlung von Mikroorganismen und Zellkulturen GmbH (Braunschweig, Germany)) and were provided in freeze-dried condition stored at −75 °C. *E. coli* is a standard Gram-negative laboratory microorganism, which is responsible for many diarrheal diseases, and is therefore well suited as reference bacterium for disinfecting water [2,14]. Gram-positive *B. subtilis*, on the other hand, is used as an additional reference microorganism, which delivers further information about the disinfection process with and without total reflection in comparison to *E. coli* [4,15]. Due to structural differences in the construction and composition of their membrane, Gram-negative microorganisms tend to show increased susceptibility to UVC radiation [16,17]. *B. subtilis* strains were applied in their vegetative state and not as spores for all experiments in this study. All bacterial strains were cultivated aerobically in Luria-Bertani (LB) broth consisting of distilled water, 10 g/L NaCl, 5 g/L yeast extract, and 10 g/L tryptone. Growth phase was realized using the incubator TH30 from Edmund Buehler GmbH (Hechingen, Germany) at 120 rpm and 37 °C for *E. coli* and 30 °C for *B. subtilis* over a period of 24 h, until stationary phase was reached. Initial concentration of this culture after 24 h was determined at 10^9 CFU/mL (*E. coli*, $OD_{600nm} = 0.76$) and 10^8 CFU/mL (*B. subtilis*, $OD_{600nm} = 0.53$) by spectrometry

referenced on LB broth at 600 nm. Finally, bacterial cultures were inoculated into sterile 0.9% saline solution to a final concentration of approximately $1–3 \times 10^6$ CFU/mL. For *B. subtilis* 1 mL of the initial solution was diluted with 100 mL of 0.9% saline solution.

2.3. Analysis Methods—Recovery and Enumeration of Bacteria

Disinfection rates were measured by membrane filtration as described by DIN EN ISO 8199:2007 [18,19]. In this method, microorganisms are collected on a membrane filter and incubated on a specific nutrient pad (Endo for *E. coli*, Caso for *B. subtilis*, both from Sartorius (Goettingen, Germany)). In order to enumerate viable microorganisms, each sample was six-fold serially diluted in 0.9% saline solution and filtered. Colonies were counted after incubation for 24 h at 37 °C (*E. coli*) and 30 °C (*B. subtilis*). All experiments were performed in triplicate. The actual concentration of microorganisms inside a bacterial solution was then calculated by Equation (1), leaving the weighted average of the counting from each experiment expressed in CFU per mL as a result [19].

$$N = \frac{Z}{V_{\text{tot}}} \times V_{\text{S}} = \frac{Z}{\sum_i n_i V_i d_i} \times V_{\text{S}} \tag{1}$$

N: Number of CFU/mL;

n_i: Number of filters per dilution i;

Z: Sum of counted colonies on filters with different dilutions d_1, d_2, …;

V_{S}: Reference volume, here: 1 mL;

V_i: Volume per dilution i;

V_{tot}: Sum of all used reference volumes.

The colony count range for valid results was set from 10 to 200 colonies, discarding filters with a higher or lower number of colonies. Before each disinfection process, the concentration of the initial stock solution N_0 was measured by filtration as described above. The inactivation rate was furthermore determined by dividing the filtered concentration of the initial stock solution N_0 by the evaluated bacterial concentration N_i after defined time intervals t_i of 10, 40, and 90 s of UVC irradiation. The overall logarithmic inactivation rate was finally determined by calculating $\log_{10} \frac{N_i}{N_0}$ [20]. Additionally, standard deviation was calculated between the three singly verified inactivation rates of each experiment with Excel® (Microsoft, Redmond, WA, USA).

2.4. Output Power and Wavelength of UVC Light Source

Important features of the applied UVC light source are the actual output power and the emission wavelength peak, which set disinfection capabilities. The actual wavelength peak of the OPTAN280J UVC-LED [12] was determined by an Avaspec 2048 XL CCD spectrometer from Avantes (Apeldoorn, The Netherlands) at 281.8 nm and can be seen in Figure 3. The Avaspec 2048 spectrometer measures incoming photons in digitally recorded counts (ADC) according to an adjusted integration time (here: 50 μs) and, therefore, only delivers relative values visualizing the wavelength peak of this LED and not the overall output power.

Additional absolute values for the emitted optical radiant output power are delivered by measurements with an OPM150 power meter from Qioptics (Goettingen, Germany). Over a defined time

interval of 90 s, a slight degradation (from 1.04 mW to 0.95 mW) of the LED output power was observed, leading to an average power output of 0.97 mW. In the datasheet, the overall radiant output of this LED type is defined between 1–2 mW and, therefore, corresponds to the measured value here [12]. This value will also be the referenced as UVC power for the following experiments which leads to an overall UVC dose of 77.82 mJ/cm^2 for 90 s.
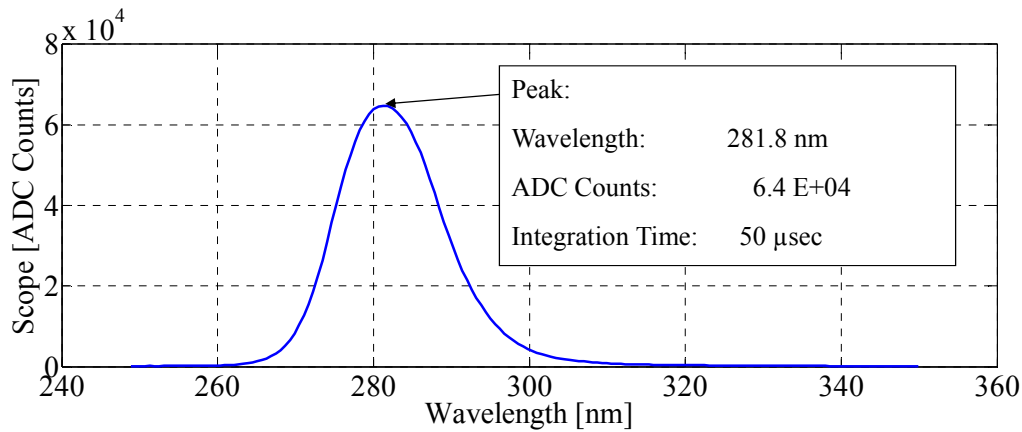

Figure 3. Measured spectrum of OPTAN280J UVC-LED from 250 to 350 nm in ADC (analogue to digital converted) counts.

2.5. Investigation of Quartz as Light Guide for UVC radiation

Transmission spectra for HSQ® 100 quartz and soda-lime AR® glass are critical parameters for describing the actual light guidance effect. Therefore, the transmission curves for the applied quartz and soda-lime glass were measured with a Specord 250 Plus spectrophotometer from Analytik Jena (Jena, Germany). Figure 4 shows these measured transmissions in a wavelength range from 200 nm to 450 nm referenced on air.
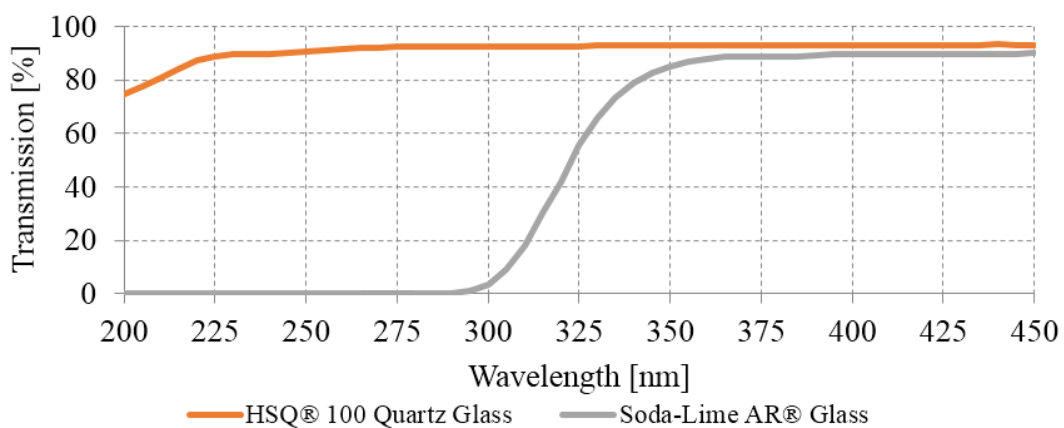

Figure 4. Transmission of HSQ® 100 quartz glass (red) (92% at 280 nm) and soda-lime glass (green) (2% at 280 nm) with a thickness of 1 mm between 200 and 450 nm; reference: air.

Soda-lime AR® glass has a transmission rate of 2% at 280 nm. On the other hand, HSQ® 100 quartz transmits 92% of the incoming UVC radiation in this wavelength. In practice, the strong absorbance of soda-lime glass would mean losing optical power at the reactor walls. Thus, 90% of UVC radiation

impinging the glass walls could theoretically be saved by HSQ® 100 due to these measured high transmittance characteristics.

Further considerations are taken into account for describing reflection and transmission properties of UVC inside a quartz glass tube. The general optical equations (Snell's law (Equation (2)) and Fresnel laws) are valid here and allow the calculation of reflectance of UVC at different media interfaces [9]. For getting a better understanding, Figure 5 represents a schematic view of the investigated problem description with interfaces from water to quartz and from quartz to water. Additionally, the refraction indexes of the different media of water, quartz, and air are depicted.
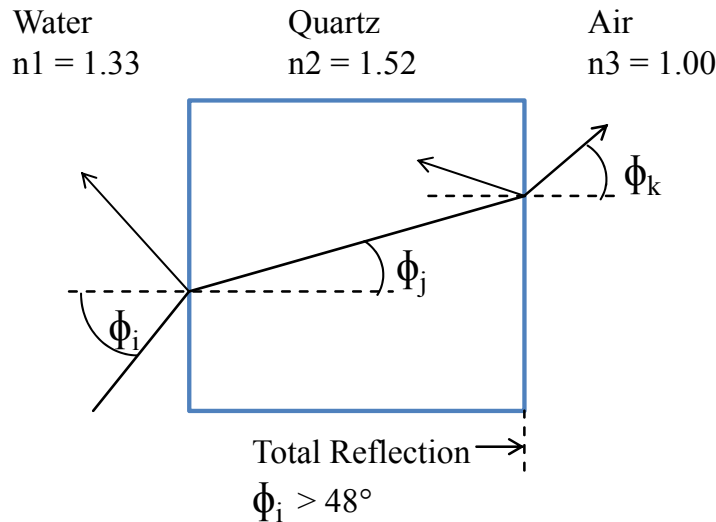

Figure 5. Optical reflection characteristics at water-quartz and quartz-air interfaces.

The incident angle is described by Φ_i and the refraction angles by Φ_j, Φ_k, which can be calculated by Snell's law [9]:

$$\sin \Phi_i * n_i = sin \Phi_j \times n_j \tag{2}$$

Φ_i: Incident angle (°);
n_i: Refraction index of medium i;
Φ_j: Angle of refraction (°);
n_j: Refraction index of medium j.

which leads to [9]

$$\Phi_j = \arcsin(\frac{n_1}{n_2} \times \Phi_i) \tag{3}$$

$$\Phi_k = \arcsin(\frac{n_1}{n_3} \times \Phi_j) \tag{4}$$

Reflection and transmission characteristics from water to quartz as well as from quartz to air are calculated by Fresnel's equations [9] and plotted in Figure 6.

According to these results, the total reflection at the quartz-air transition is given for incident angles Φ_i greater than 48°. Radiation impinging the quartz surface at a lower incident angle will be emitted almost completely on the outside and will be lost for disinfection. However, the applied UVC-LED has a viewing angle of 15° and, therefore, total reflection at the quartz walls can be ensured.
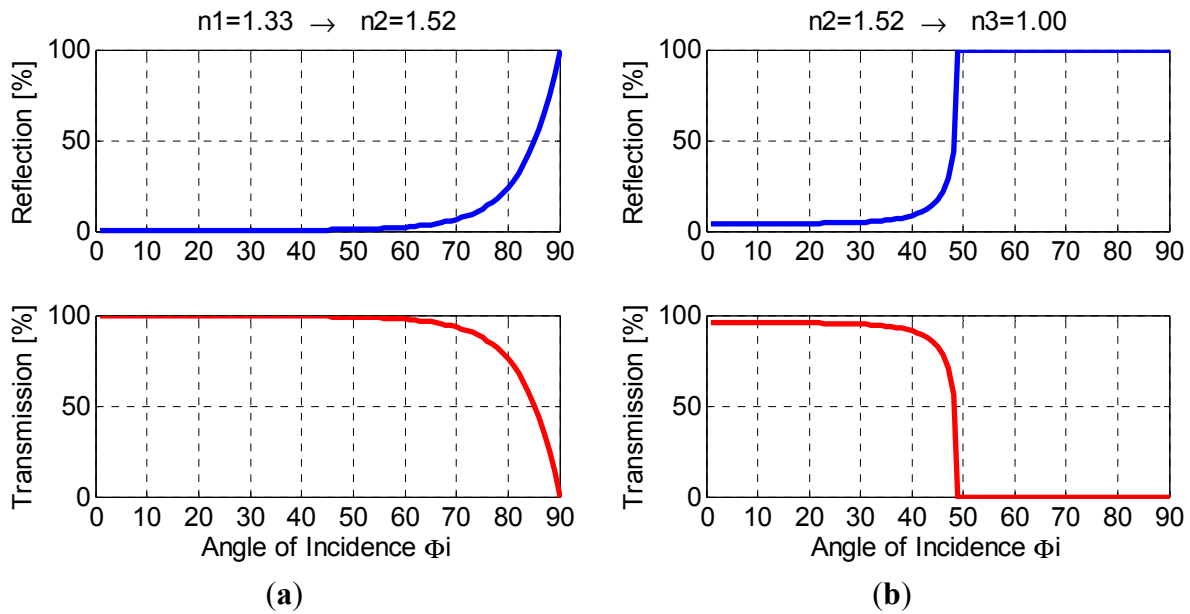
Figure 6. (**a**) Reflection and transmission from water to quartz with incident angles at the water-quartz interface Φ_i of 0° to 90°; (**b**) resulting reflection and transmission from quartz to air observed for incident angles at the water-quartz interface Φ_i of 0° to 90°.

2.6. Absorbance Characteristics of UVC radiation in Different Media

One concern with UVC radiation is its strong attenuation, especially in polluted water. This effect has a direct influence on the evaluated reactor design with quartz tubes and is therefore very important in this scientific study. The attenuation of UVC inside a medium can be explained theoretically by Equation (5) [21]:

$$I(z) \ = \ I_0 \times 10^{-c\varepsilon z} \tag{5}$$

$I(z)$: Beam intensity at distance z from radiating source (W/cm^2);

I_0: Initial intensity at $z = 0$ (W/cm^2);

c: Concentration of absorbing molecule (mol/L);

z: Layer thickness (cm);

ε: Molar extinction coefficient (L/(mol·cm)).

which leads to the formulation of Beer's law [9,22]

$$\log_{10}\left(\frac{I(z)}{I_0}\right) \ = \ c\varepsilon z \ = \ A \tag{6}$$

A: Absorption (L/cm).

If monochromatic and collimated light passes through a homogeneous medium, the incident light is absorbed in proportion to the distance z from the radiating light source. Attenuation of I_0 then follows Equation (6) and is dependent on the layer thickness z and a material-specific extinction coefficient $c\varepsilon$ [21]. Extinction ratio $c\varepsilon z$ is also referred to as absorption A or optical density OD.

The absorption of the investigated bacteria media determines how deep UVC radiation is able to penetrate the cultivated bacteria solution. The measured absorbance of the applied *B. subtilis*, *E. coli*,

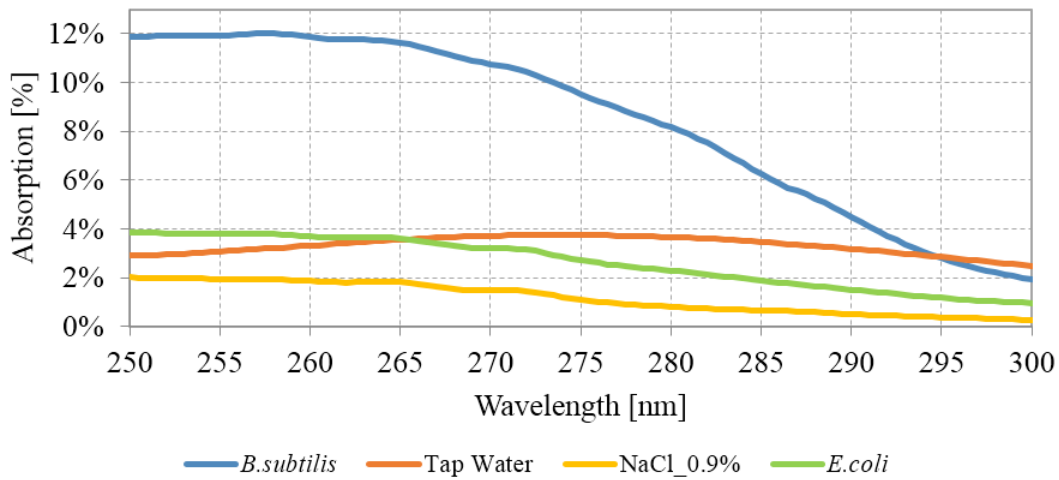0.9% NaCl solution, and tap water referenced on distilled water from 250 nm to 300 nm can be seen in Figure 7.

Figure 7. Absorption of tap water (region: Ulm, Germany), 0.9% NaCl solution, *E. coli* DSM 498, and *B. subtilis* DSM 402 solution (1–3 × 10^6 CFU/mL; 0.9% NaCl, distilled water); reference: pure water; layer thickness: 10 mm.

In Figure 8, resulting fluence rates of UVC through a defined medium are calculated by applying extinction coefficients (*c*ε) of 0.023 (~*E. coli* solution (10^6 CFU/mL)), 0.037 (~tap water from Ulm, Germany), and 0.081 (~*B. subtilis* solution (10^6 CFU/mL)) at a varying layer thickness z from 0 mm to 100 mm, neglecting scattering effects. Equation (5) delivers attenuation as described by Beer's law. The resulting fluence rate can be derived by taking the irradiated area into account, which is determined by the LED's viewing angle of 15° and the layer thickness z. Effects of total reflection (quartz) and absorbance (soda-lime) are recognizable as soon as the irradiated area reaches the inner area of the tubes.

$$r = z \times \tan\frac{\alpha}{2} \qquad (7)$$

$$A = \pi \times r^2 \rightarrow F = \frac{I(z)}{A} \qquad (8)$$

r: Radius of irradiated area (cm);
α: LED viewing angle (°);
A: Irradiated area (cm^2);
F: Fluence (mW/cm^2).

As consequence of UVC attenuation, according to Beer's law, a high extinction coefficient prevents the radiation from entering deep into the media and the investigated light guide effect of quartz glass is severely restricted. An extinction coefficient below 0.1 would theoretically be a realistic absorbance range for average tap water quality, which also corresponds to the findings here [23,24].

According to Li *et al.*, a high reflection coefficient at the inner wall of an UVC reactor can lead to an increased weighted average in fluence rate [13]. The calculations from Figure 8 correspond to these findings.

Another issue is the interaction of UVC radiation with solid particles [25], causing scattering effects or delivering shaded areas for microorganisms, which reduces disinfection efficiency and disturbs the

light guide effect as well. Figure 9 gives a summary of the possible interactions with solid particles concerning UVC disinfection according to Blume *et al.* [26].
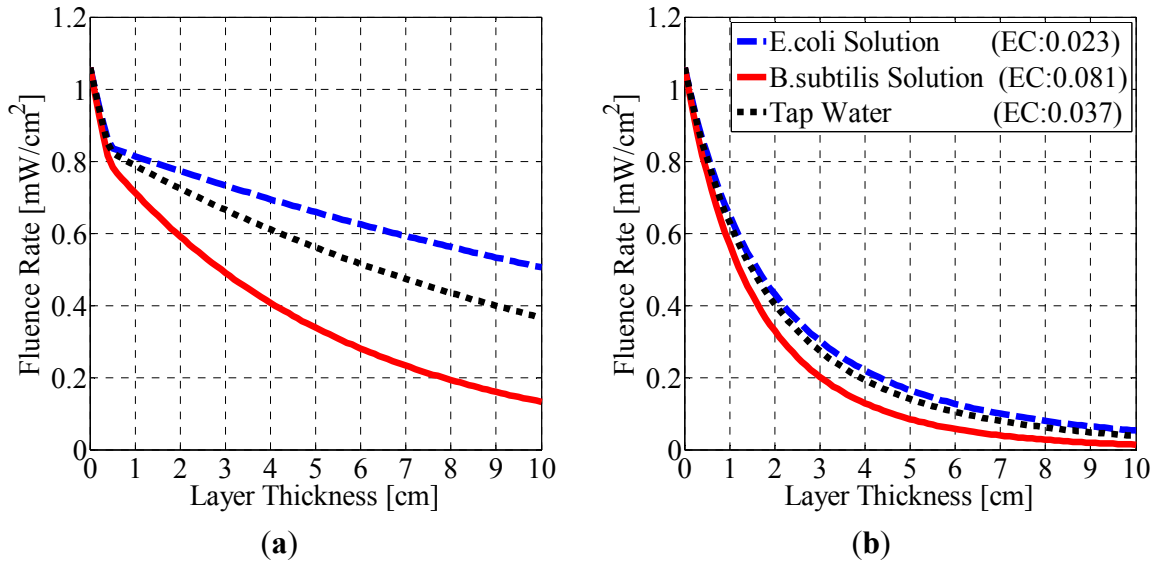

(**a**)   (**b**)

Figure 8. Calculated fluence rate of UVC radiation (280 nm) applying Beer's law with different extinction coefficients (EC): EC: 0.023 (*E. coli* solution), EC: 0.081 (*B. subtilis* solution), and EC: 0.037 (tap water). UVC power: 0.97 mW; LED viewing angle: 15° (**a**) with total reflection; (**b**) without total reflection.
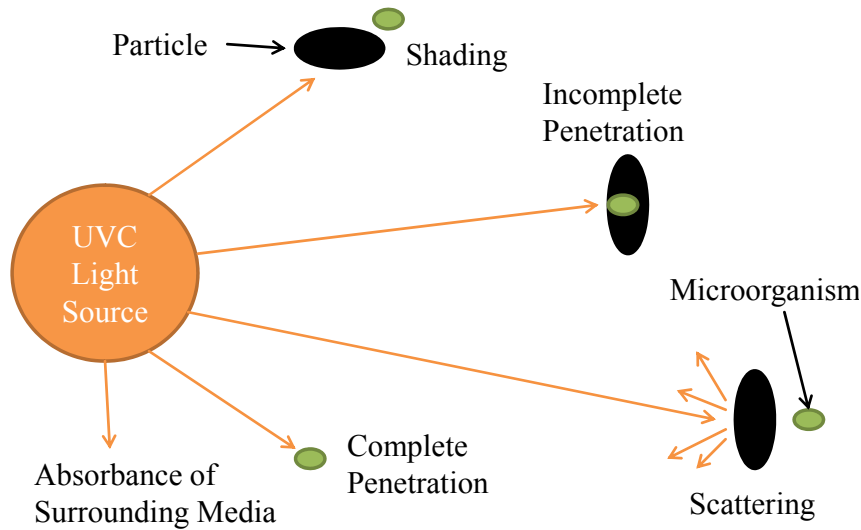

Figure 9. Particle interactions with UVC radiation inside a medium.

Thus, the theoretical basic conditions disclose that the highest inactivation rates can be achieved in a medium that has low absorbance and contains only little solid particles. Both of these demands could be met by a pre-switched filtering system, for example.

3. Results and Discussion

3.1. Disinfection Results for E. coli DSM 498 and B. subtilis DSM 402 in Stagnant Bacteria Solution

Figure 10 shows the evaluated inactivation rates for *B. subtilis* DSM 402 with UVC irradiation periods of 10 s, 40 s, and 90 s, comparing quartz glass and soda-lime glass without additional mixing of the samples during the experiments. The initial *B. subtilis* concentration N_0 of the samples was determined at $1–3 \times 10^6$ CFU/mL. Additionally, the corresponding regression line as well as the correlation coefficients of each disinfection process, evaluated with Excel®, are given. Standard deviation is marked with error bars.
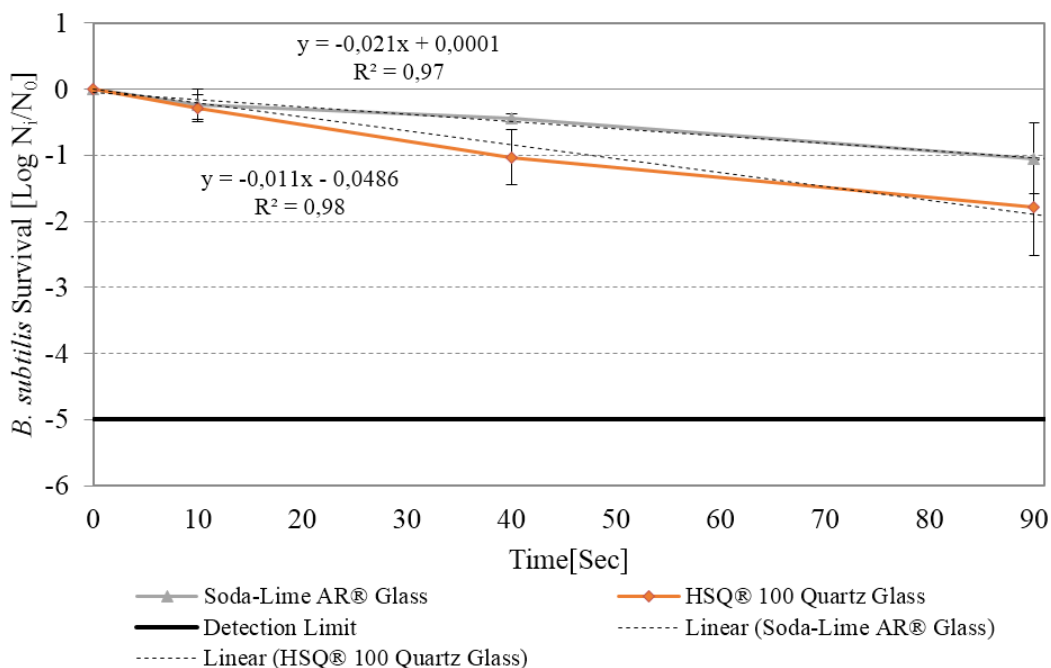

Figure 10. Disinfection results in $\log_{10}$ for *B. subtilis* ($1–3 \times 10^6$ CFU/mL) without additional mixing during UVC irradiation.

The overall $\log_{10}$ inactivation of *B. subtilis* reached from 1.04 $\log_{10}$ (soda-lime glass) to 1.79 $\log_{10}$ (quartz glass) after 90 s of UVC irradiation. Quantifiable differences of the inactivation efficiency between soda-lime and quartz glass were determined at 0.06 $\log_{10}$ (10 s), 0.57 $\log_{10}$ (40 s), and 0.75 $\log_{10}$ (90 s). The numerical values and the corresponding standard deviation for the data shown in Figure 10, as well as the differences in disinfection efficiency between the two glass types, can be seen in Table 1.

Table 1. Inactivation results for HSQ® 100 and AR® glass types for *B. subtilis* DSM 402 after different UVC irradiation periods and the corresponding differences of microbial inactivation in $\log_{10}$ in stagnant samples.

UVC Irradiation/s	$\log_{10} \frac{N_i}{N_0}$—HSQ® 100 Glass	$\log_{10} \frac{N_i}{N_0}$—AR® Glass	Difference/$\log_{10}$
10	0.29 ± 0.20	0.23 ± 0.23	0.06 ± 0.43
40	1.03 ± 0.41	0.46 ± 0.06	0.57 ± 0.47
90	1.79 ± 0.72	1.04 ± 0.49	0.75 ± 1.21

The results for the stagnant experiments applying *E. coli* DSM 498 can be seen in Figure 11 as well as Table 2. The initial *E. coli* concentration N_0 of the samples was also determined at $1-3 \times 10^6$ CFU/mL for all experiments.

Quartz glass shows higher inactivation rates of 0.35 $\log_{10}$ (10 s), 0.53 $\log_{10}$ (40 s), and 0.95 $\log_{10}$ (90 s) in the experiments, with inactivation results up to 2.80 $\log_{10}$ (quartz glass) and 1.85 $\log_{10}$ (soda-lime glass) after 90 s of UVC irradiation.
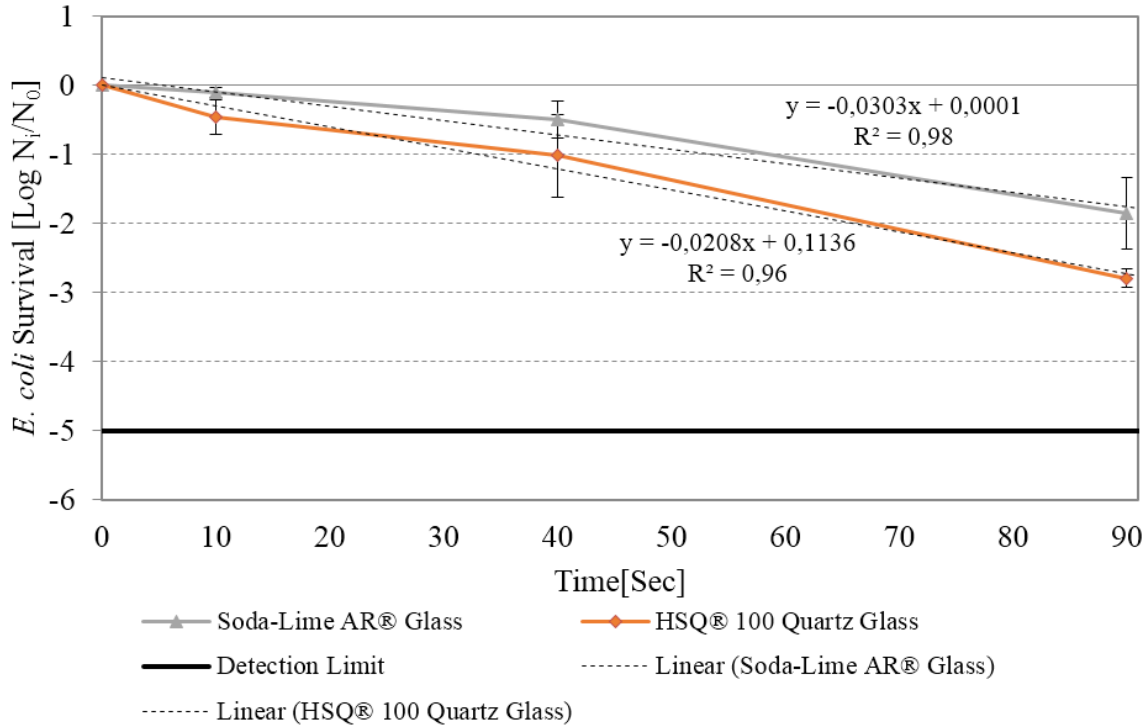

Figure 11. Disinfection results in $\log_{10}$ for *E. coli* ($1-3 \times 10^6$ CFU/mL) without additional mixing during UVC irradiation.

Table 2. Inactivation results for HSQ® 100 and AR® glass types for *E. coli* DSM 498 after different UVC irradiation periods and the corresponding differences of microbial inactivation in $\log_{10}$ in stagnant samples.

UVC Irradiation/s	$\log_{10}\frac{N_i}{N_0}$—HSQ® 100 Glass	$\log_{10}\frac{N_i}{N_0}$—AR® Glass	Difference/$\log_{10}$
10	0.46 ± 0.25	0.11 ± 0.06	0.35 ± 0.31
40	1.02 ± 0.60	0.49 ± 0.27	0.53 ± 0.87
90	2.80 ± 0.13	1.85 ± 0.51	0.95 ± 0.64

3.2. Disinfection Results with E. coli DSM 498 and B. subtilis DSM 402 in Mixed Bacteria Solution

The same experiments were carried out with continuous mixing of the samples during UVC irradiation. The results from Figure 12 show higher disinfection rates compared to the previous results without mixing. An overall reduction for *E. coli* of 1.21 $\log_{10}$ (soda-lime glass) and 4.28 $\log_{10}$ (quartz glass) after 40 s was observed. The investigated difference between quartz and soda-lime glass is 0.74 $\log_{10}$ (10 s) and 3.07 $\log_{10}$ (40 s). After 90 s, all filters for the disinfection experiments with quartz glass contained

zero colonies and were therefore under the detection limit of 10^1 CFU/mL. The highest disinfection rate for soda-lime glass was measured at 2.59 $\log_{10}$ after 90 s of UVC irradiation.

A summary of all evaluated $\log_{10}$ inactivation rates and the corresponding standard deviation during this experiment are given in Table 3. There are noticeable improvements in *E. coli* inactivation with HSQ$^®$ 100 glass in comparison to AR$^®$ glass up to 3.07 $\log_{10}$.

The corresponding results for *B. subtilis* from Figure 13 and Table 4 support these results. Here, the overall reduction was determined at 2.47 $\log_{10}$ (soda-lime glass) and 3.86 $\log_{10}$ (quartz glass) after 90 s UVC-treatment. Increased inactivation rates of 0.29 $\log_{10}$ (10 s), 1.59 $\log_{10}$ (40 s), and 1.39 $\log_{10}$ (90 s) for quartz glass were measured uniformly during the experiment.
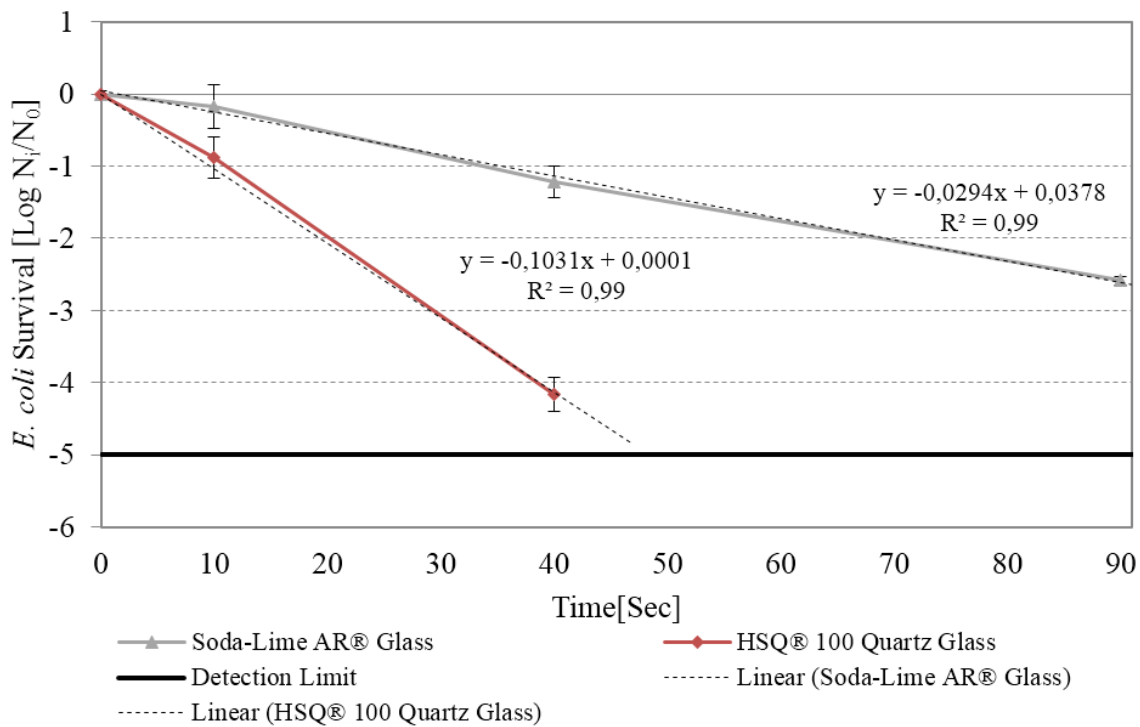

Figure 12. Disinfection results expressed in $\log_{10}$ levels for *E. coli* (1–3×10^6 CFU/mL) with additional mixing during UVC irradiation.

Table 3. Inactivation results for HSQ$^®$ 100 and AR$^®$ glass types for *E. coli* DSM 498 after different UVC irradiation periods and the corresponding differences of microbial inactivation in $\log_{10}$ in mixed samples.

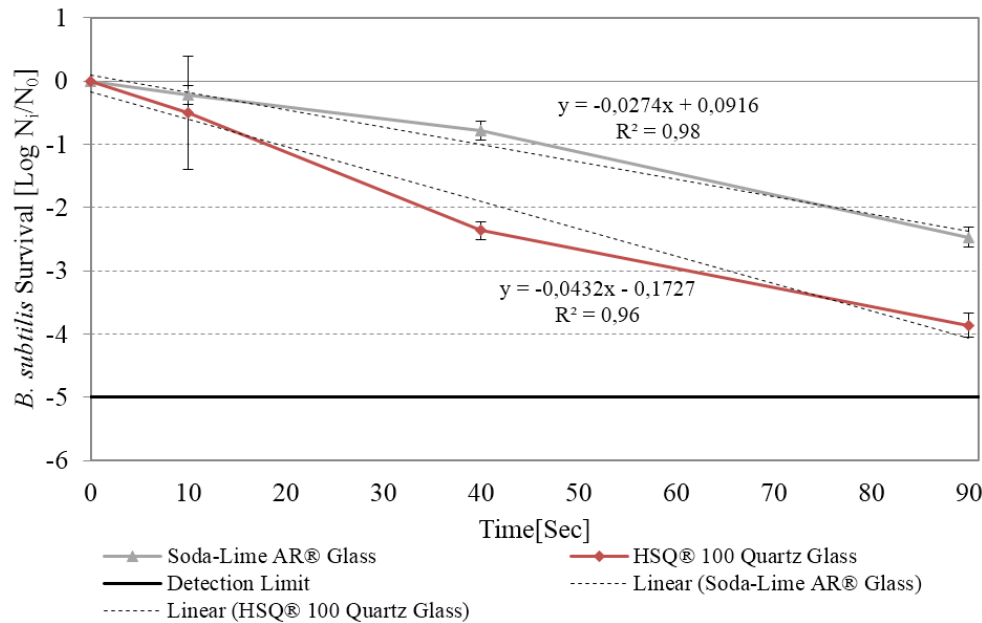| UVC Irradiation/s	$\log_{10} \frac{N_i}{N_0}$—HSQ$^®$ 100 Glass	$\log_{10} \frac{N_i}{N_0}$—AR$^®$ Glass	Difference/$\log_{10}$
10	0.91 ± 0.21	0.17 ± 0.30	0.74 ± 0.51
40	4.28 ± 0.37	1.21 ± 0.22	3.07 ± 0.59
90	>5.00	2.59 ± 0.05	>2.41

Figure 13. Disinfection results expressed in $\log_{10}$ levels for *B. subtilis* ($1–3 \times 10^6$ CFU/mL) with additional mixing during UVC irradiation.

Table 4. Inactivation results for HSQ® 100 and AR® glass types for *B. subtilis* DSM 402 after different UVC irradiation periods and the corresponding differences of microbial inactivation in $\log_{10}$ in mixed samples.

UVC Irradiation/s	$\log_{10}\frac{N_i}{N_0}$—HSQ® 100 Glass	$\log_{10}\frac{N_i}{N_0}$—AR® Glass	Difference/$\log_{10}$
10	0.51 ± 0.89	0.22 ± 0.14	0.29 ± 1.03
40	2.37 ± 0.13	0.78 ± 0.15	1.59 ± 0.28
90	3.86 ± 0.19	2.47 ± 0.16	1.39 ± 0.35

Thus, the overall inactivation rate in the mixed disinfection experiments with *B. subtilis* was increased by quartz glass as well. However, the investigated differences between inactivation efficiency with and without the light guide approach are lower compared to the results with *E. coli*. All numerical inactivation results are highlighted in Table 4.

Uniformly increased disinfection rates are visible for both bacterial strains by utilizing quartz instead of soda-lime glass. This outcome indicates that the light guide effects for UVC disinfection deliver strong improvements in disinfection efficiency with UVC-LEDs of several $\log_{10}$ levels, especially in mixed samples.

4. Conclusions

Quartz tubes applied as light guides for UVC disinfection allow harvesting almost all of the incoming UVC power and using it for disinfection due to total reflection. A clearly visible difference could be identified between stagnant and mixed samples during UVC irradiation here. This difference could be explained by the mentioned attenuation of UVC radiation along the tube and the absorption and total reflection at the reactor walls, respectively. With this method, only the upper part of the bacteria sample is exposed to these high doses of nearly 80 mJ/cm^2 if there is no mixing during the experiment. The

fluence rate decreases by 65% in the investigated *B. subtilis* solution and by 55% in the *E. coli* solution after a layer thickness of just 20 mm and tends close to zero after 60 to 70 mm without total reflection (see Figure 8). In contrast, utilizing total reflection with quartz, the fluence rate drops only by 40% (*B. subtilis* solution) and 22% (*E. coli* solution) after a layer thickness of 20 mm. The higher disinfection rates for quartz glass are therefore most likely caused by the slower descent of fluence along the tube and the resulting increase of the UVC dose. However, the disinfection results with stagnant bacteria samples show only minor improvements in efficiency with the light guide approach. Furthermore, as a consequence of these similar disinfection capabilities, the error bars of the calculated standard deviation partly overlap. Therefore, no clear improvements between quartz glass and soda-lime glass can be observed for the stagnant experiments in practical use. All experiments were repeated with additional mixing, showing much higher disinfection rates for both bacterial strains. By mixing, all bacteria contained in the irradiated samples were driven close to the UVC-LED and were therefore exposed to a much higher dose than without mixing. This effect can clearly be seen in the experiments. *B. subtilis* strains were more resistant to UVC radiation throughout the experiments than *E. coli*, which is most likely caused by the mentioned different Gram stain of both microorganisms [16,17]. The quartz and, thus, the light guide concept showed higher disinfection rates of up to 3.07 $\log_{10}$ (*E. coli*) after 40 s of UVC irradiation and 1.39 $\log_{10}$ (*B. subtilis*) after 90 s of UVC irradiation. A strong improvement in disinfection efficiency from applying quartz as a light guide can be verified here in comparison to soda-lime glass. These results suggest that this concept is best suited for flow reactor designs in practical use. Because of the limited radiant output power of today's UVC-LEDs, which is usually less than 3 mW, and the high cost of at least several hundred dollars, the concept of total reflection could improve the profitability of such a system. Furthermore, a geometry that is able to homogenize the incoming radiation inside the tube could offer even more advantages. A possible way of circumventing the strong absorbance would be to couple UVC with UVA-LEDs. This combination showed increased disinfection results according to Chevremont *et al.* [20].

Author Contributions

Andrej Gross was mainly responsible for drawing up the paper and planning the experimental setups. Felix Stangl and Katharina Hoenes performed bacterial experiments, countings, and interpretations of the microbial results. Martin Hessling and Michael Sift set up the basic idea of this novel reactor design using light guide effects of quartz glass and delivered important information concerning optical and microbial questions that were used in this study. Furthermore, Michael Sift designed optical simulations which served as basis for the simulations in this paper.

Conflicts of Interest

The authors declare no conflict of interest.

References

1. United Nations Educational, Scientific, and Cultural Organization (UNESCO). *Water and Energy: The United Nations World Water Development Report 2014*; UNESCO: Paris, France, 2014.
2. Ashbolt, N.J. Microbial contamination of drinking water and disease outcomes in developing regions. *Toxicology* **2004**, *198*, 229–238.
3. Lui, G.Y.; Roser, D.; Corkish, R.; Ashbolt, N.; Jagals, P.; Stuetz, R. Photovoltaic powered ultraviolet and visible light-emitting diodes for sustainable point-of-use disinfection of drinking waters. *Sci. Total Environ.* **2014**, *493*, 185–196.
4. U.S. Environmental Protection Agency, Office of Water. *Ultraviolet disinfection guidance manual for the final Long Term 2 Enhanced Surface Water Treatment Rule*; U.S. Environmental Protection Agency, Office of Water: Washington, DC, USA, 2006.
5. Gray, N.F. Chapter Thirty-Four Ultraviolet Disinfection. In *Microbiology of Waterborne Diseases Microbiological Aspects and Risks*; Academic Press: Waltham, MA, USA, 2014; pp. 617–630.
6. Kowalski, W.J. *Ultraviolet Germicidal Irradiation Handbook: UVGI for Air and Surface Disinfection*; Springer-Verlag: Heidelberg, Germany, 2009.
7. Jagger, J. *Introduction to Research in Ultraviolet Photobiology*; Prentice-Hall: Englewood Cliffs, NJ, USA, 1967.
8. Stangl, F.; Gross, A.; Hoenes, K.; Sift, M.; Schlau, D.; Hessling, M. Advanced Photovoltaic Water Disinfection System Based on Efficient UVC and Ultrasound Generation. In Proceedings of the 4rd Symposium Small PV Applications, Messegelände, Germany, 9–10 June 2015; pp. 86–91.
9. Bolton, J.R. Calculation of ultraviolet fluence rate distributions in an annular reactor: Significance of refraction and reflection. *Water Res.* **2000**, *34*, 3315–3324.
10. Oguma, K.; Kita, R.; Sakai, H.; Murakami, M.; Takizawa, S. Application of UV light emitting diodes to batch and flow-through water disinfection systems. *Desalination* **2013**, *328*, 24–30.
11. Jenny, R.M.; Simmons, O.D.; Shatalov, M.; Ducoste, J.J. Modeling a continuous flow ultraviolet Light Emitting Diode reactor using computational fluid dynamics. *Chem. Eng. Sci.* **2014**, *535*, 524–535.
12. CrystalIS. *Optan—High Performance UVC LEDs for Instrumentation*; CrystalIS: Green Island, NY, USA, 2014.
13. Li, M.; Qiang, Z.; Bolton, J.R.; Ben, W. Impact of reflection on the fluence rate distribution in a UV reactor with various inner walls as measured using a micro-fluorescent silica detector. *Water Res.* **2012**, *46*, 3595–3602.
14. Kamanula, J.F.; Zambasa, O.J.; Masamba, W.R. Quality of drinking water and cholera prevalence in Ndirande Township, City of Blantyre, Malawi. *Phys. Chem. Earth A/B/C* **2014**, *72*, 61–67.
15. Chang, J.C.; Ossoff, S.F.; Lobe, D.C.; Dorfman, M.H.; Dumais, C.M.; Qualls, R.G.; Johnson, J.D. UV inactivation of pathogenic and indicator microorganisms. *Appl. Environ. Microbiol.* **1985**, *49*, 1361–1365.
16. Williams, P.D.; Eichstadt, S.L.; Kokjohn, T.A.; Martin, E.L. Effects of Ultraviolet Radiation on the Gram-positive marine bacterium Microbacterium maritypicum. *Curr. Microbiol.* **2007**, *55*, 1–7.
17. Rai, V.R. *Microbial Food Safety and Preservation Techniques*; CRC Press: Boca Raton, FL, USA, 2015.

18. Gordalla, B. 3.11 Standardized Methods for Water-Quality Assessment. In *Treatise on Water Science*; Elsevier: Amsterdam, The Netherlands, 2013; pp. 263–302.

19. DIN Deutsches Institut für Normung e.V. *Water Quality—General Guidance on the Enumeration of Microorganisms by Culture*; DIN EN ISO 8199:2007; Beuth: Berlin, Germany 2008.

20. Chevremont, A.-C.; Farnet, A.-M.; Coulomb, B.; Boudenne, J.-L. Effect of coupled UV-A and UV-C LEDs on both microbiological and chemical pollution of urban wastewaters. *Sci. Total Environ.* **2012**, *426*, 304–310.

21. Larsen, M.L.; Clark, A.S. On the link between particle size and deviations from the Beer–Lambert–Bouguer law for direct transmission. *J. Quant. Spectrosc. Radiat. Transf.* **2014**, *133*, 646–651.

22. Maikala, R.V. Modified Beer's Law—Historical perspectives and relevance in near-infrared monitoring of optical properties of human tissue. *Int. J. Ind. Ergon.* **2010**, *40*, 125–134.

23. U.S. Environmental Protection Agency, Office of Water. *Guidance Manual for Conducting Sanitary Surveys of Public Water Systems: Surface Water and Ground Water under the Direct Influence (GWUDI) of Surface Water*; U.S. Environmental Protection Agency, Office of Water: Washington, DC, USA, 1999.

24. Pope, R.M.; Fry, E.S. Absorption spectrum (380–700 nm) of pure water. II. Integrating cavity measurements. *Appl. Opt.* **1997**, *36*, 8710–8723.

25. Jin, X.; Li, Z.; Xie, L.; Zhao, Y.; Wang, T. Synergistic effect of ultrasonic pre-treatment combined with UV irradiation for secondary effluent disinfection. *Ultrason. Sonochem.* **2013**, *20*, 1384–1389.

26. Blume, T.; Neis, U. Improved wastewater disinfection by ultrasonic pre-treatment. *Ultrason. Sonochem.* **2004**, *11*, 333–336.